CHAPTER 5

Experimental Results

5.1 Introduction

Experiments were performed according to the operating conditions summarized in Table 4.1. Physical properties of cotton fibre are shown in Appendix A. Data and calculated results are tabutated in Appendix B. The sample of calculation are shown in Appendix C.

From Table 4.1, the experiments were divided into 15 groups with the aim of varying speed of stirrer from 80-750 rpm., tension of cotton fibre from 112,380-337,130 gm/cm^2, temperature from 303-343 °K and concentration of sodium ions from $4.8 \times 10^{-3} - 1.27 \times 10^{-2}$ gm-mole/ml. For each group of these experiments, five runs were operated at different times to study the effect of these process variables on the rate of reaction, conversion and effective diffusivity of sodium ions.

5.2 Testing the Experimental Results with the Derived Theory

Considering Eqs. (3.29) and (3.32), if the variables such as D_e and $(C_{Na^+})_b$ are constant, the remaining relationship will be in terms of

$$t = f(r_1/r_{1,i}) \tag{5.1}$$

To reveal this relationship, the experiments were performed at constant $(C_{Na^+})_b$, T, S and V_e at 4.8×10^{-3} gm-mole/ml, 303°K, 112,380 gm/cm^2 and 750 rpm. respectively, the cotton yarns were mercerized at 129, 420, 643, 758 and 860 seconds, then the cross-sections were cut to determine $r_1/r_{1,i}$, the results are shown in Appendix B.3. The retationship between t and $f(r_1/r_{1,i})$ was plotted on the common scale as shown in Figs. 5.1 and 5.2. The experimental results were fit very well with Eq. (3.32), it can be concluded that the rate of mercerization process is controlled by diffusion of sodium ions through the alkali cellulose. Thus the knowledge of D_e is essential in order to predict the global rate.

5.3 Influence of Process Variables on the Relationship between t and $\left[1 - (r_1/r_{1,i})^2 \left(1\text{-}\ln (r_1/r_{1,i})^2\right)\right]$

Since the rate of the reaction is controlled by diffusion of sodium ions through alkali-cellulose so that the relationship between t and $\left[1\text{-}(r_1/r_{1,i})^2 \left(1\text{-}\ln(r_1/r_{1,i})^2\right)\right]$ will be linear according to Eq. (3.32). The experiments were performed by varying the process variables to see their effects on the relationship between t and $\left[1\text{-}(r_1/r_{1,i})^2 \left(1\text{-}\ln(r_1/r_{1,i})^2\right)\right]$.

5.3.1 Influence of stirring speed

The relationship between t and $\left[1\text{-}(r_1/r_{1,i})^2 \left(1\text{-}\ln (r_1/r_{1,i})^2\right)\right]$ were plotted at the stirring speed of 80, 200 and 750 rpm. as shown in Fig. 5.3 The experimental results give

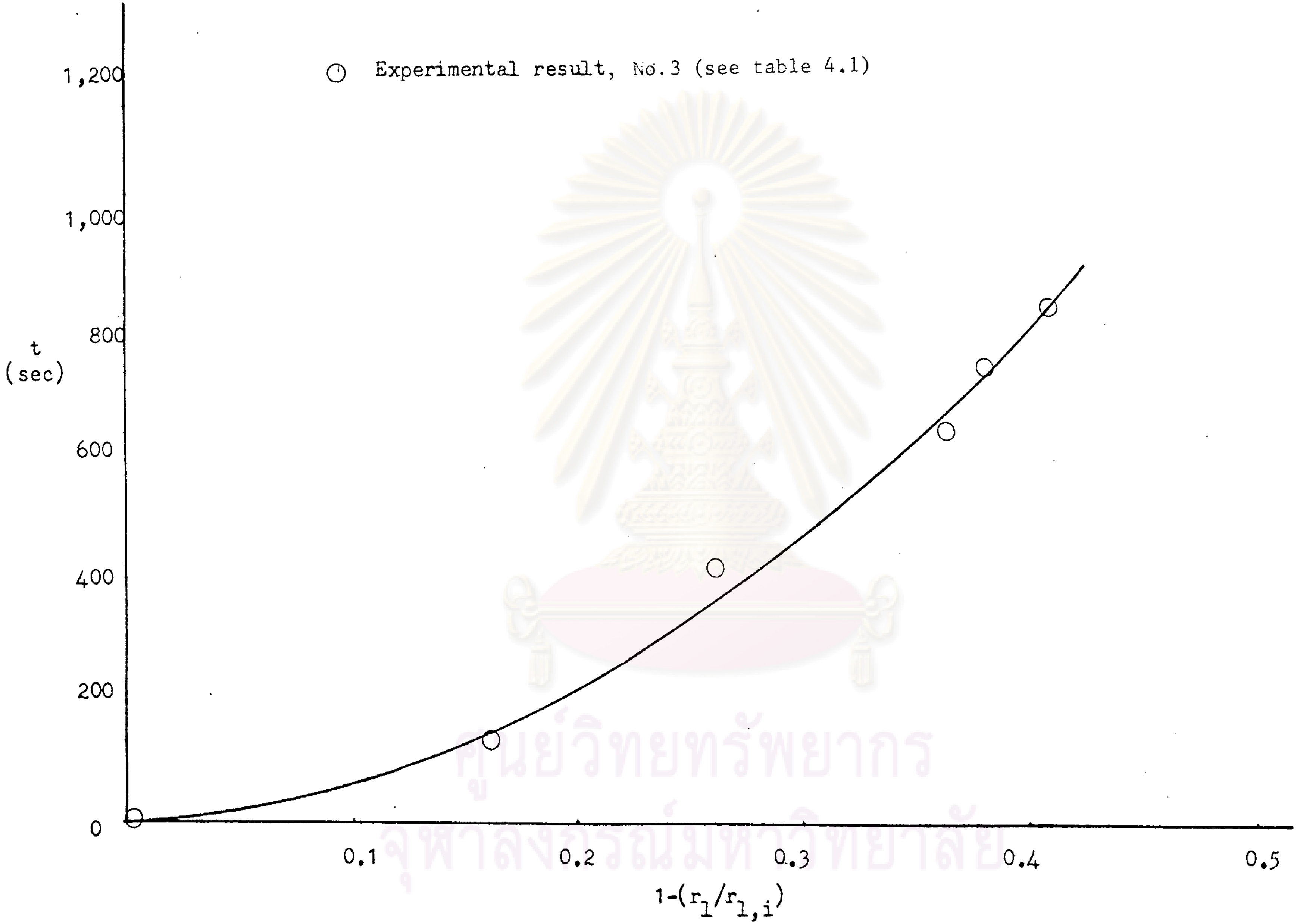

Fig. 5.1 Relationship between t and $1-(r_1/r_{1,i})$

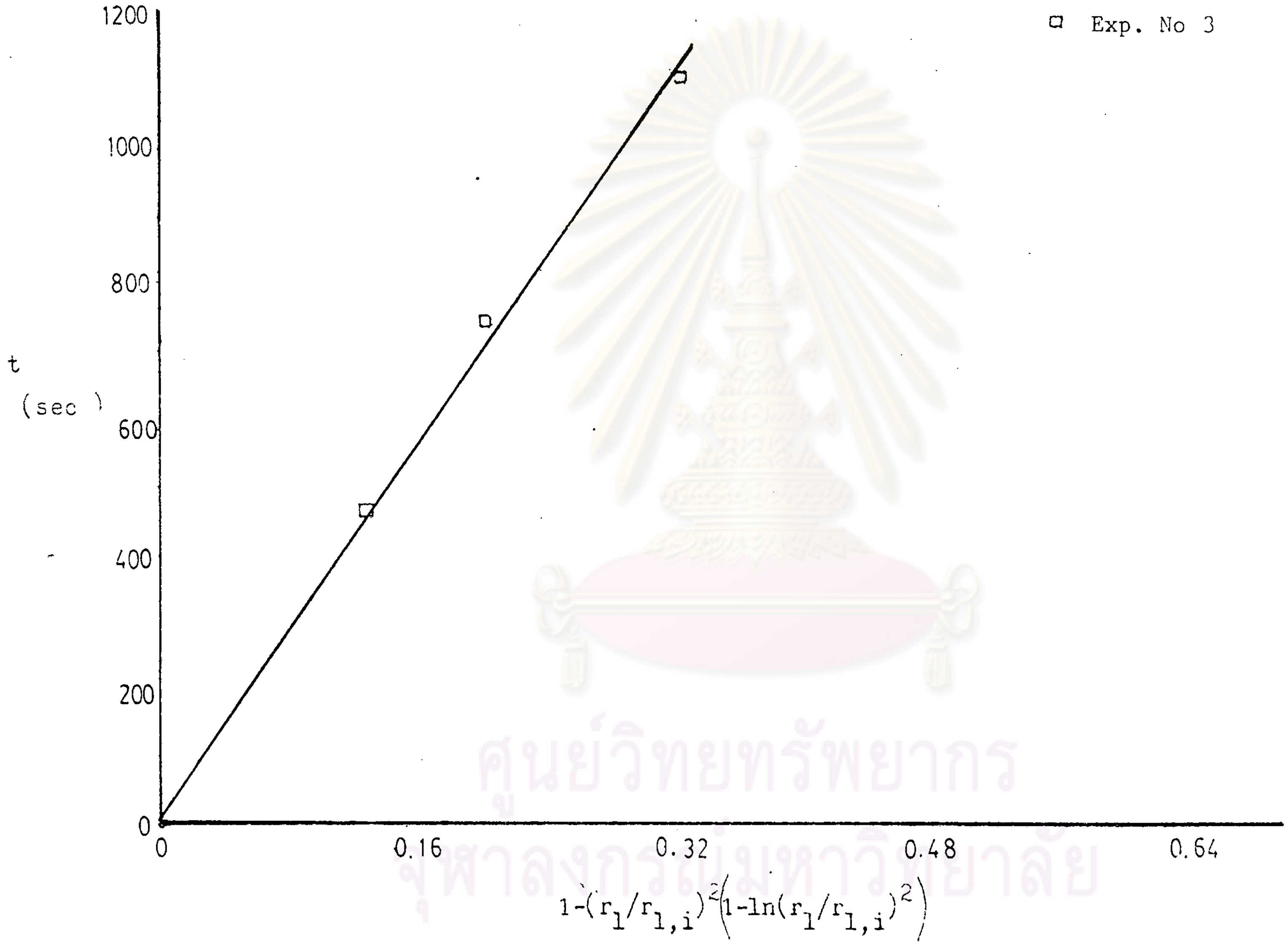

Fig. 5.2 Relationship between t and $\left[1-(r_1/r_{1,i})^2\left(1-\ln(r_1/r_{1,i})^2\right)\right]$

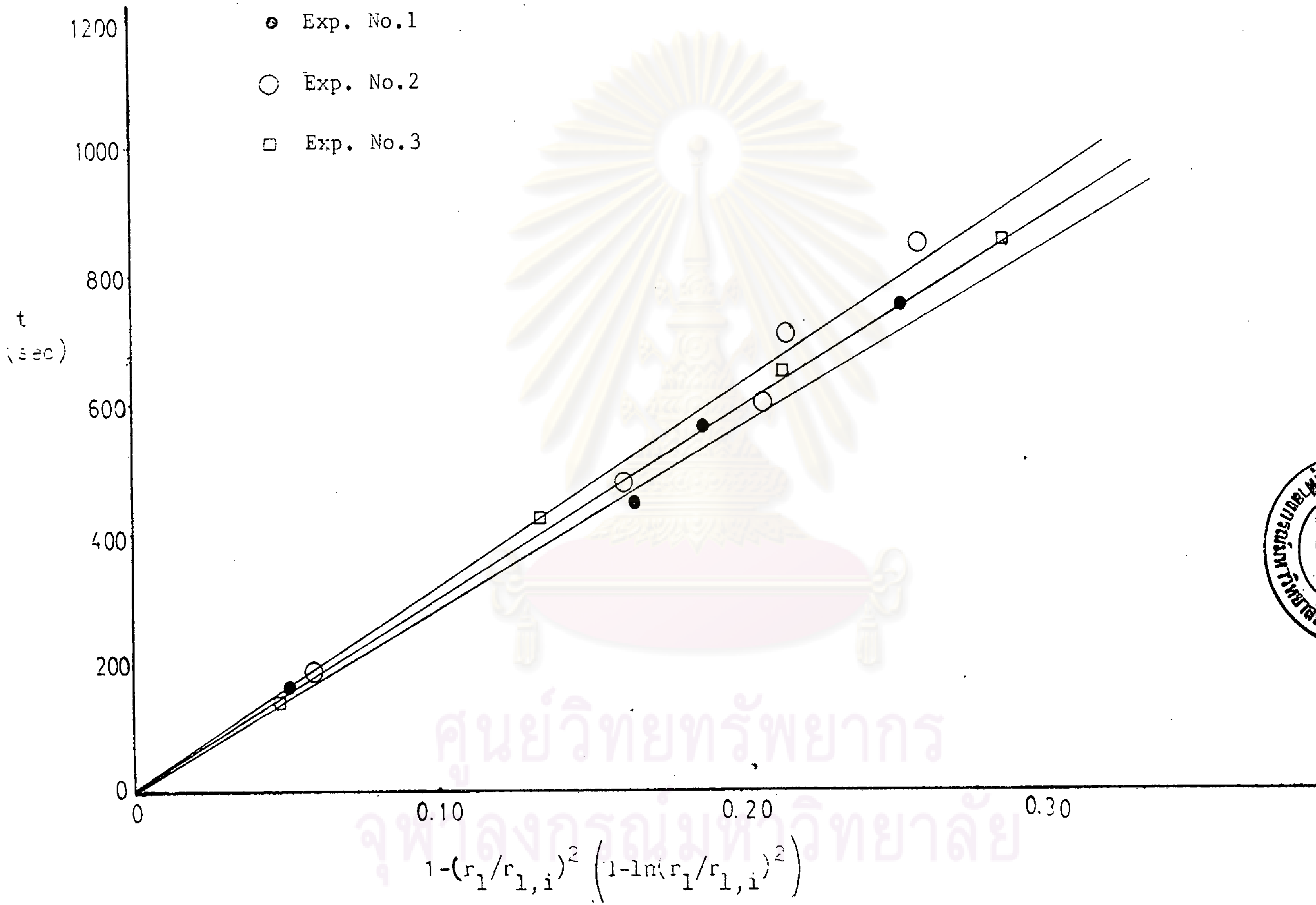

Fig. 5.3 Relationship between t and $\left[1-(r_1/r_{1,i})^2\left(1-\ln(r_1/r_{1,i})^2\right)\right]$ at various speeds of stirrer

a straight line. With the aid of the least square method, their slopes were calculated to be 3006,3206 and 3036 respectively. It is shown that there is little influence of stirring speed on the relationship between t and $\left[1-(r_1/r_{1,i})^2\left(1-\ln(r_1/r_{1,i})^2\right)\right]$ since the slope of the graph does not change when the stirring speed increases.

5.3.2 Influence of tension

The relationship between t and $\left[1-(r_1/r_{1,i})^2\left(1-\ln(r_1/r_{1,i})^2\right)\right]$ were plotted at the tension of cotton fibre of 168,560 224,755, 280,940, 337,130 gm/cm^2 as shown in Fig. 5.4. The slopes of the graphs are 3425, 3472,4524 and 5579 respectively. It is shown that the slopes of the graphs increase when the tension increases.

5.3.3 Influence of temperature

The relationship between t and $\left[1-(r_1/r_{1,i})^2\left(1-\ln(r_1/r_{1,i})^2\right)\right]$ were plotted at the temperature of 313,323, 333, 343°K as shown in Fig. 5.5 The slopes of the graphs are 2,728, 2,139, 1790 and 1431 respectively. It is shown that the slopes of the graphs decrease when the temperature increases.

5.3.4 Influence of concentration,

The relationship between t and $\left[1-(r_1/r_{1,i})^2\left(1-\ln(r_1/r_{1,i})^2\right)\right]$ were plotted at the concentration of 1.27×10^{-2}, 1.06×10^{-2}, 7.96×10^{-3} and 5.92×10^{-3} gm-mole/ml. as shown in Fig. 5.6 The slopes of the graphs are 1035, 1302, 1872

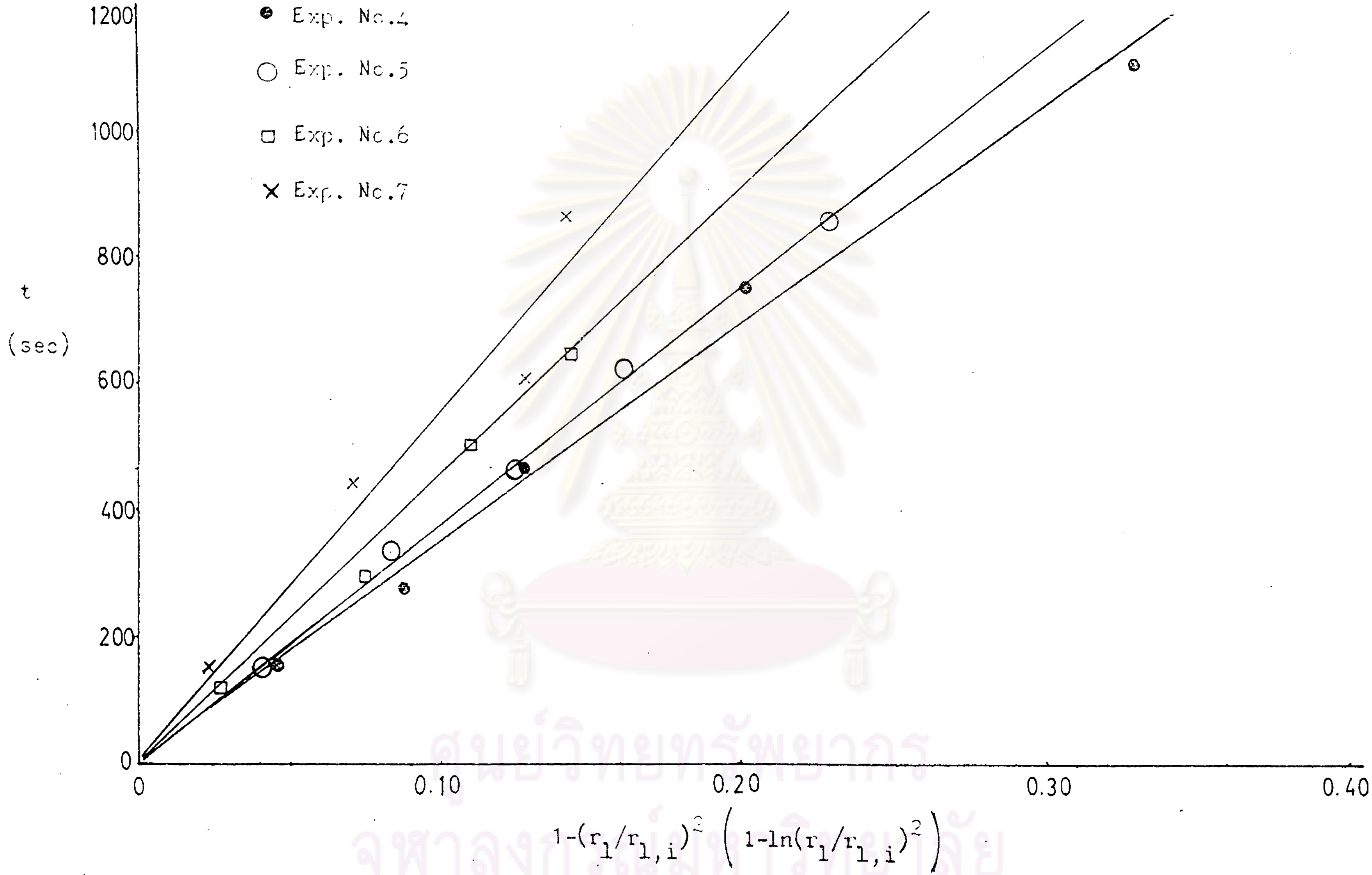

Fig. 5.4 Relationship between t and $\left[1-(r_1/r_{1,i})^2\left(1-\ln(r_1/r_{1,i})^2\right)\right]$ at various tensions of cotton fibre

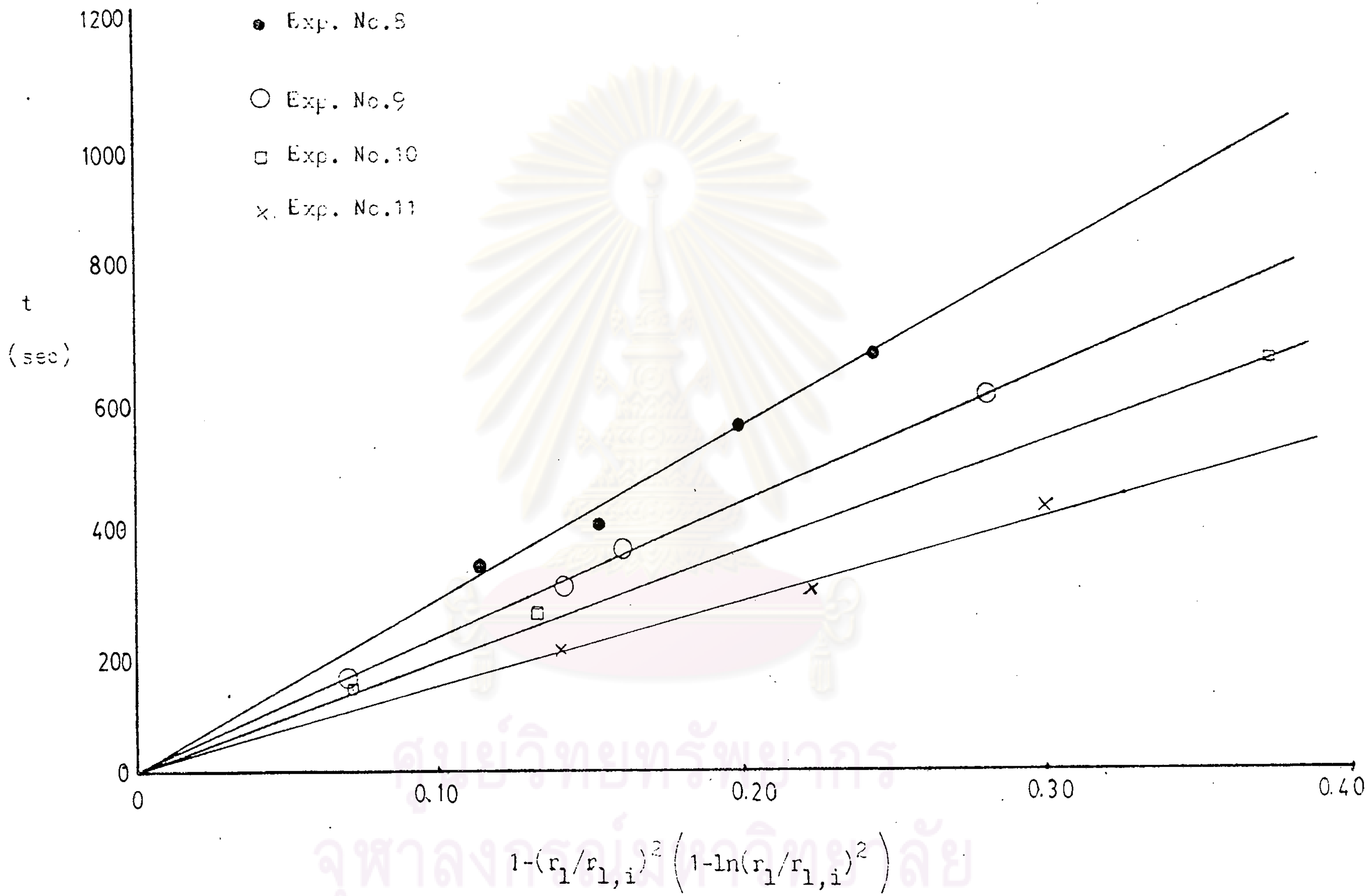

Fig. 5.5 Relationship between t and $\left[1-(r_1/r_{1,i})^2\left(1-\ln(r_1/r_{1,i})^2\right)\right]$ at various temperatures

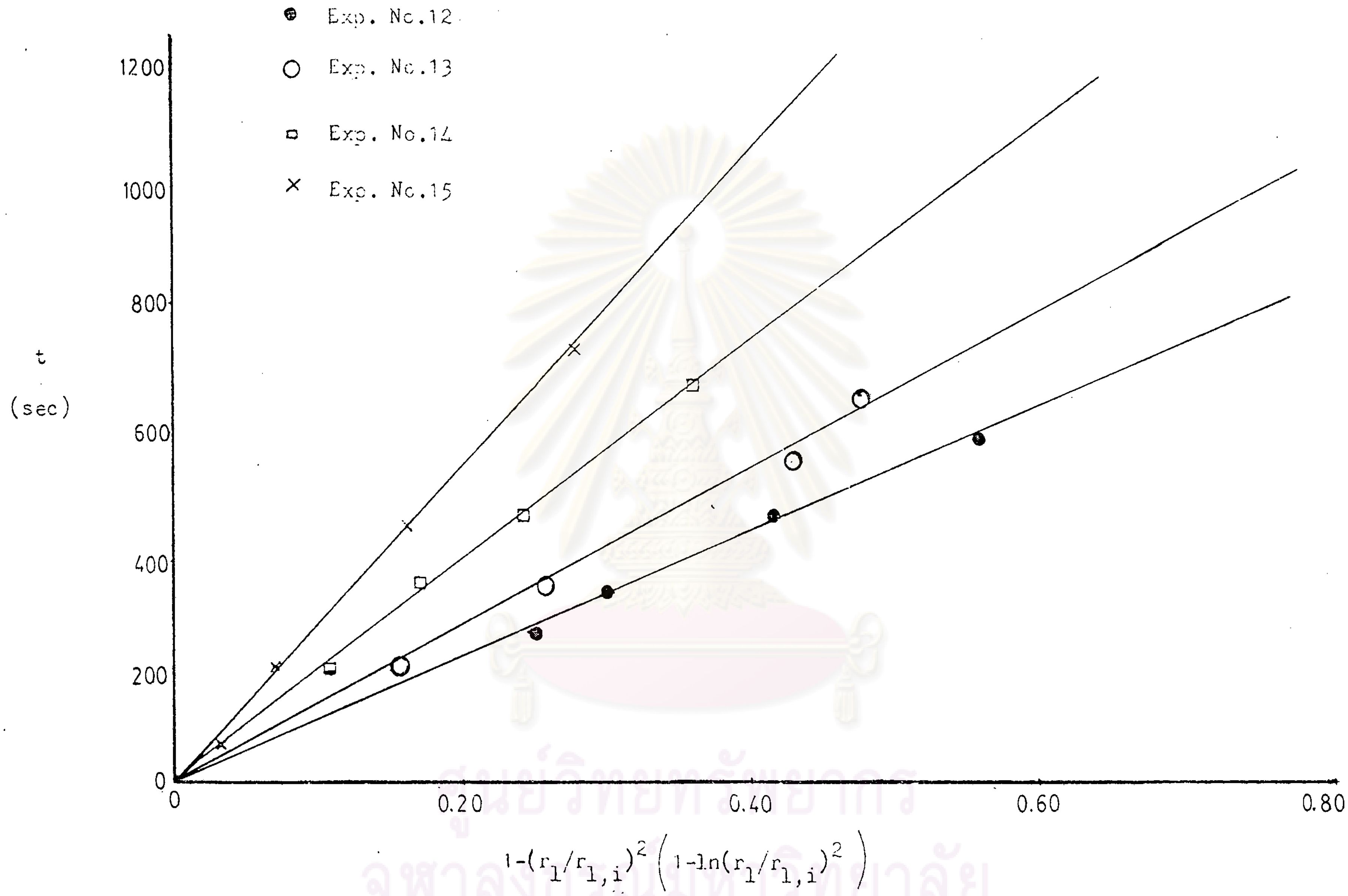

Fig. 5.6 Relationship between t and $\left[1-(r_1/r_{1,i})^2\left(1-\ln(r_1/r_{1,i})^2\right)\right]$ at various concentrations

and 2648 respectively. It is shown that the slopes of the graphs increase when the concentration of sodium ions decreases.

5.3.5 Conclusions

It was found that S,T and $(C_{Na^+})_b$ influenced on the mercerization. The next step is to find how these variables relate to the mercerization. It was found that these variables influence on the diffusivity of sodium ions in alkali-cellulose, so that D_e in Eq. (3.32) should be in terms of these variables as the following.

$$D_e = f(S, T, (C_{Na^+})_b) \tag{5.2}$$

If we can find Eq. (5.2), Eq. (3.32) will be the complete equation of mercerization.

5.4 Evaluation of Effective Diffusivity

Since the rate is controlled by diffusion of sodium ions through product alkali-cellulose so that the effective diffusivity can be calculated from Eq. (3.36). These experiments can be divided into 4 groups according to the process variables; stirring speed (V_e), tension (S), temperature (T) and concentration of sodium ions $(C_{Na^+})_b$ so that D_e can be correlated with these process variables.

5.4.1 Correlation between effective diffusivity and stirring speed

The slopes which are shown in 5.3.1 were used in calculating D_e in Eq. (3.36) and the results are shown in Appendix B.16 from which the correlation between D_e and V_e was analysed by linear regression, logarithmic regression, power regression and exponential regression to find that which regression is the best correlation between D_e and V_e by comparing correlation coefficient. The more the correlation coefficient approaches $\pm$ 1, the better the correlation between D_e and V_e (sample of calculation is shown in Appendix C). The results of regression analysis of D_e and V_e are shown in Appendix B.20 which shows that there is little correlation between D_e and V_e since its correlation coefficient is very low (<0.21). Fig. 5.7 shows the graph between D_e and V_e.

5.4.2 Correlation between effective diffusivity and tension

The slopes which are shown in paragraph 5.3.2 are used in calculating D_e in Eq. (3.36) and the results are shown in Appendix B.17 from which the correlation between D_e and S is analysed by regression analysis. The results of regression analysis are shown in Appendix B.21 which shows that linear regression is the best correlation between D_e and S, since its absolute correlation coefficient is the largest value (-0.988). The result is

$$D_e = 1.6267\times10^{-10} - 2.5112\times10^{-16}\,S$$

$$= 1.6267\times10^{-10}\,(1-1.5437\times10^{-6}S) \quad (5.3)$$

or $$D_e \;\alpha\; (1-1.5437\times10^{-6}\,S) \quad (5.4)$$

Fig. 5.8 shows the graph between D_e and S.

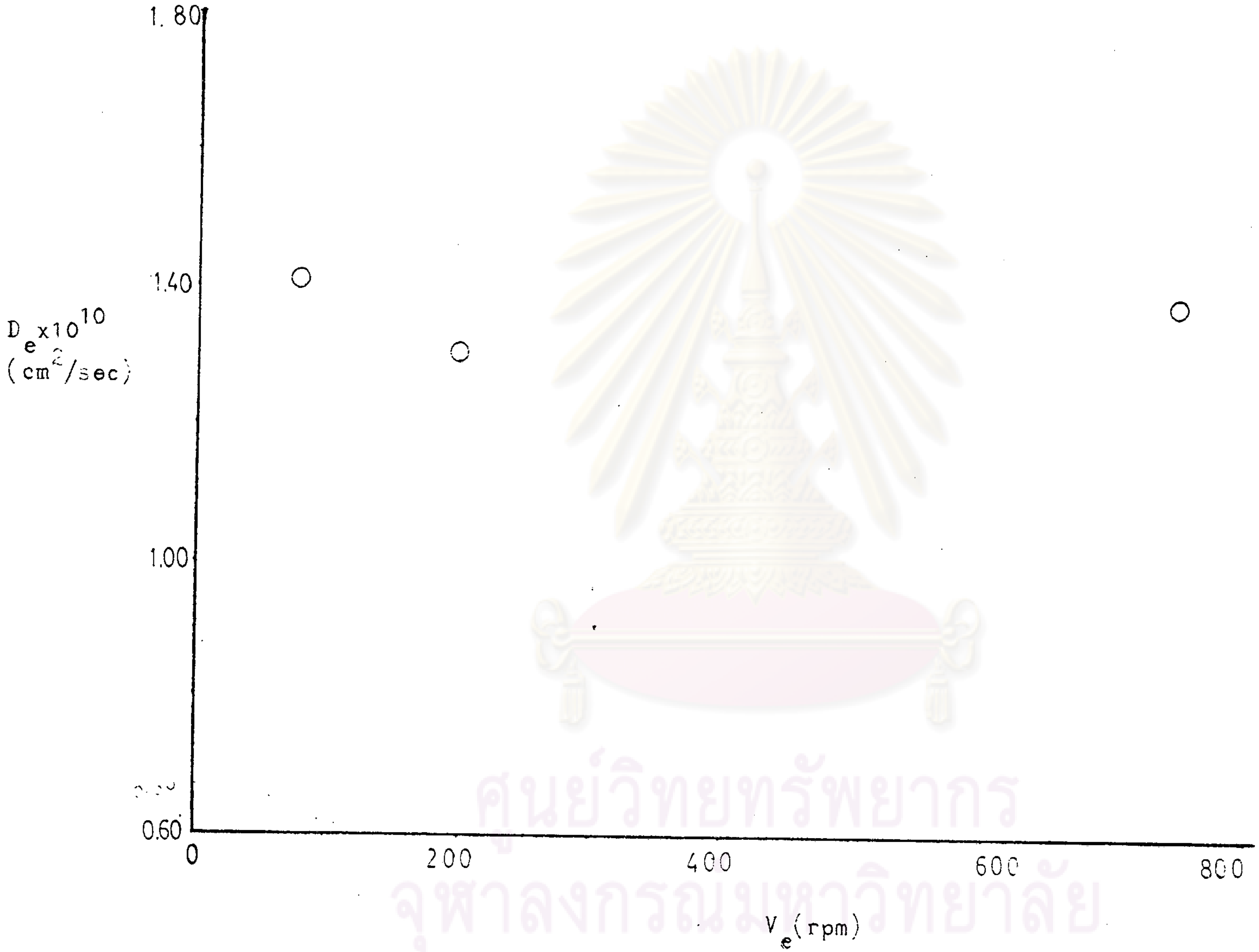

Fig. 5.7 Relationship between D_e and V_e

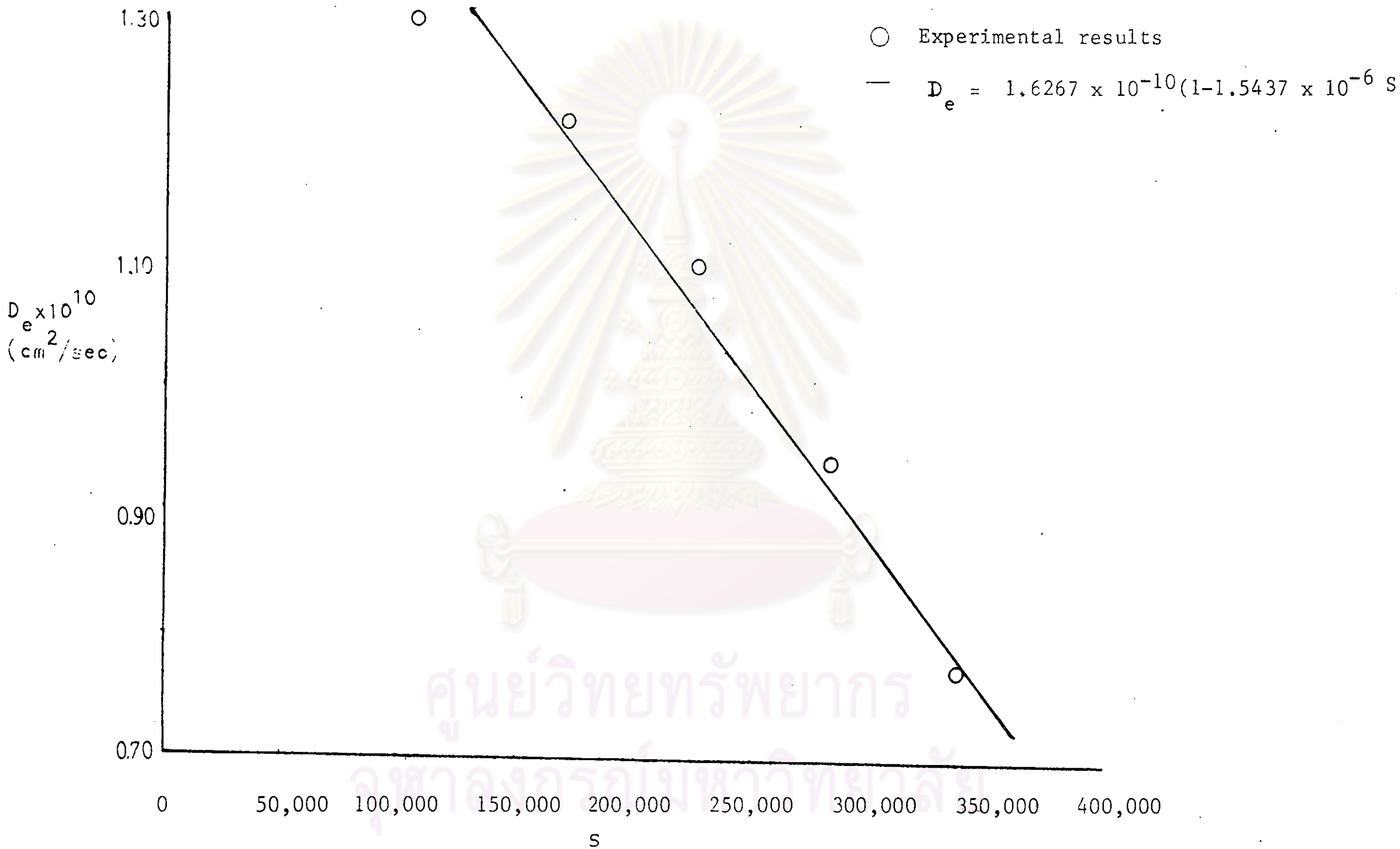

Fig. 5.8 Relationship between D_e and S

5.4.3 Correlation between effective diffusivity and temperature

The slopes which are shown in paragraph 5.3.3 are used in calculating D_e in Eq. (3.36) and the result are shown in Appendix B.18 from which the correlation between D_e and T is analysed by regression analysis. The results of regression analysis are shown in Appendix B.22 which shows that exponential regression is the best correlation between D_e and T, since its correlation coefficient is the largest value (0.999). The result is

$$D_e = 1.7058 \times 10^{-13} e^{0.0217T} \tag{5.5}$$

or

$$D_e \propto e^{0.0217T} \tag{5.6}$$

Fig. (5.9) shows the graph between D_e and T.

5.4.4 Correlation between effective diffusivity and concentration

The slopes which are shown in paragraph 5.3.4 are used in calculating D_e in Eq. (3.36) and the result are shown in Appendix B.19 from which the correlation between D_e and $(C_{Na^+})_b$ is analysed by regression analysis. The results of regression analysis are shown in Appendix B.23 which shows that power regression is the best correlation between D_e and $(C_{Na^+})_b$ since it correlation coefficient is the largest value (0.999). The result is

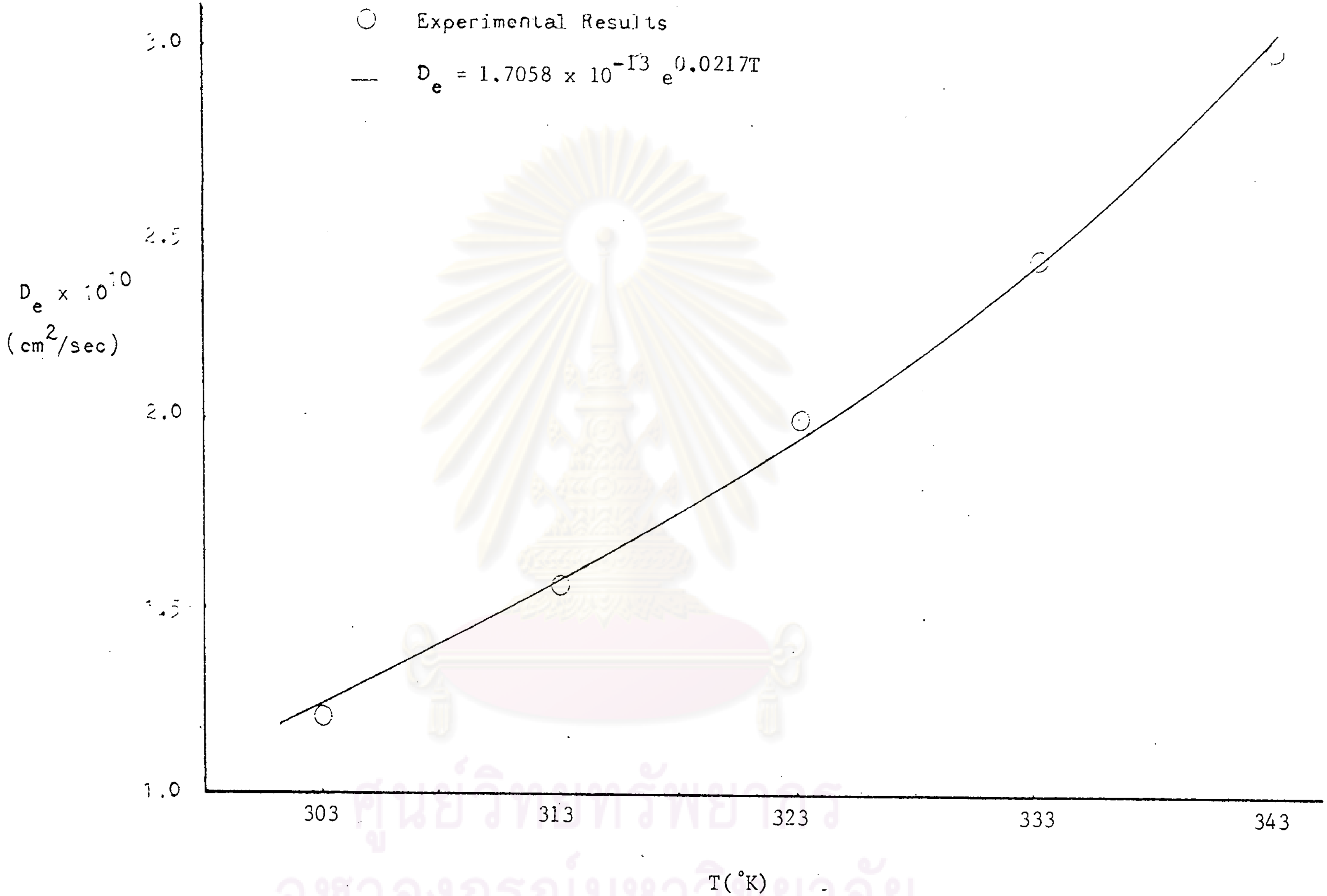

Fig. 5.9 Relationship between D_e and T

$$D_e = 4.1012 \times 10^{-10} (C_{Na^+})_b^{0.227} \tag{5.7}$$

$$D_e \propto (C_{Na^+})_b^{0.227} \tag{5.8}$$

Fig. (5.10) shows the graph between D_e and $(C_{Na^+})_b$.

5.4.5 Equation of effective diffusivity

Proportions (5.4), (5.6) and (5.8) are combined together to give the complete equation of effective diffusivity as shown below

$$D_e = K(1-1.5437 \times 10^{-6}S)\ e^{0.0217T}(C_{Na^+})_b^{0.227} \tag{5.9}$$

K in Eq. (5.8) was determined by plotting the graph between De and $(1-1.5437 \times 10^{-6}S)\ e^{0.0217T}\ (C_{Na^+})_b^{0.227}$ as shown in Fig.5.11, the slope of the graph is K which can be calculated as shown in Appendix C.7. Its value is 7.8167×10^{-13}, Upon substituting , it gives

$$D_e = 7.8167 \times 10^{-13}(1-1.5437 \times 10^{-6}S)\ e^{0.0217T}\ (C_{Na^+})_b^{0.227} \tag{5.10}$$

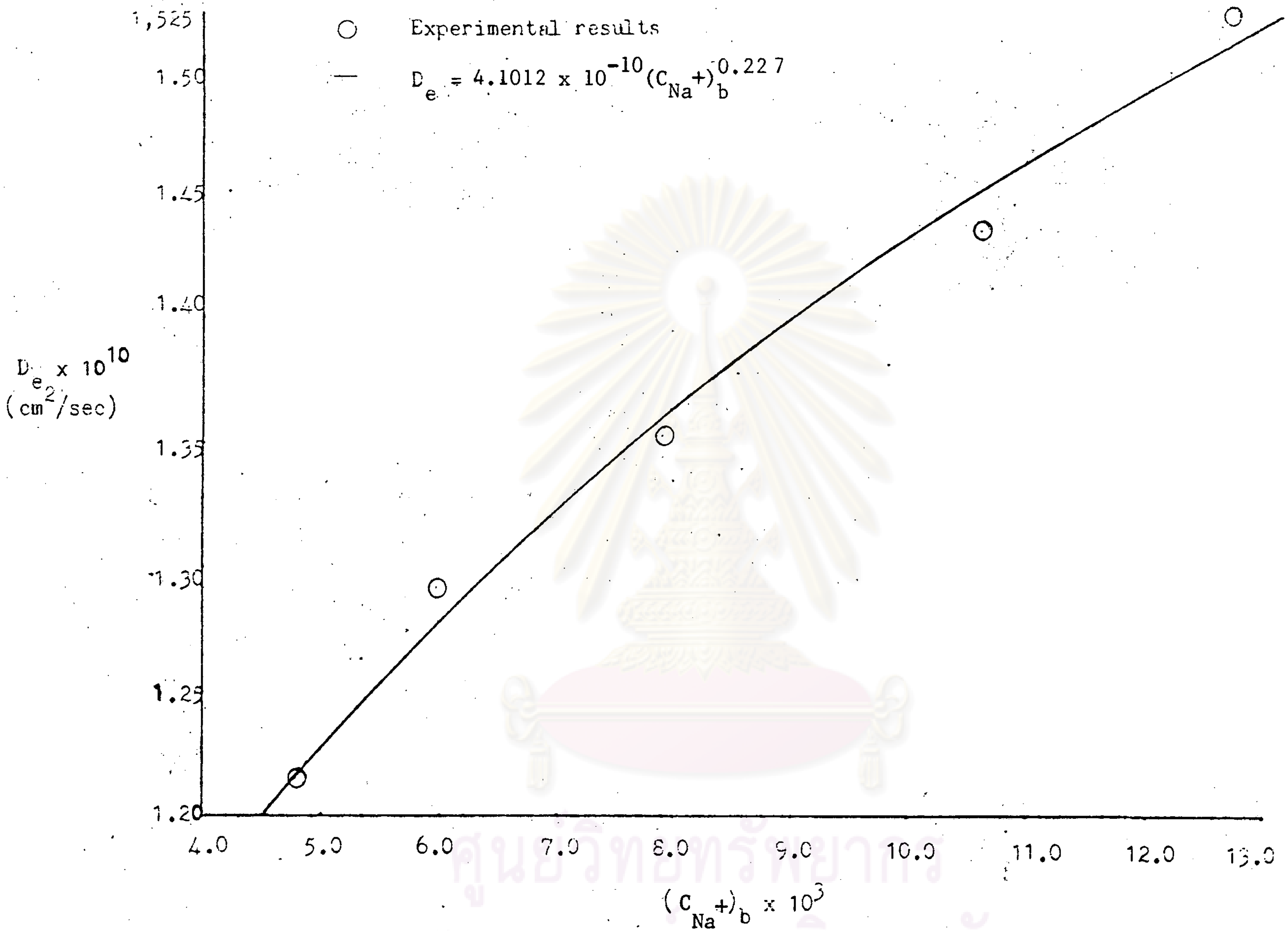

Fig 5.10 Relationship between D_e and $(C_{Na^+})_b$

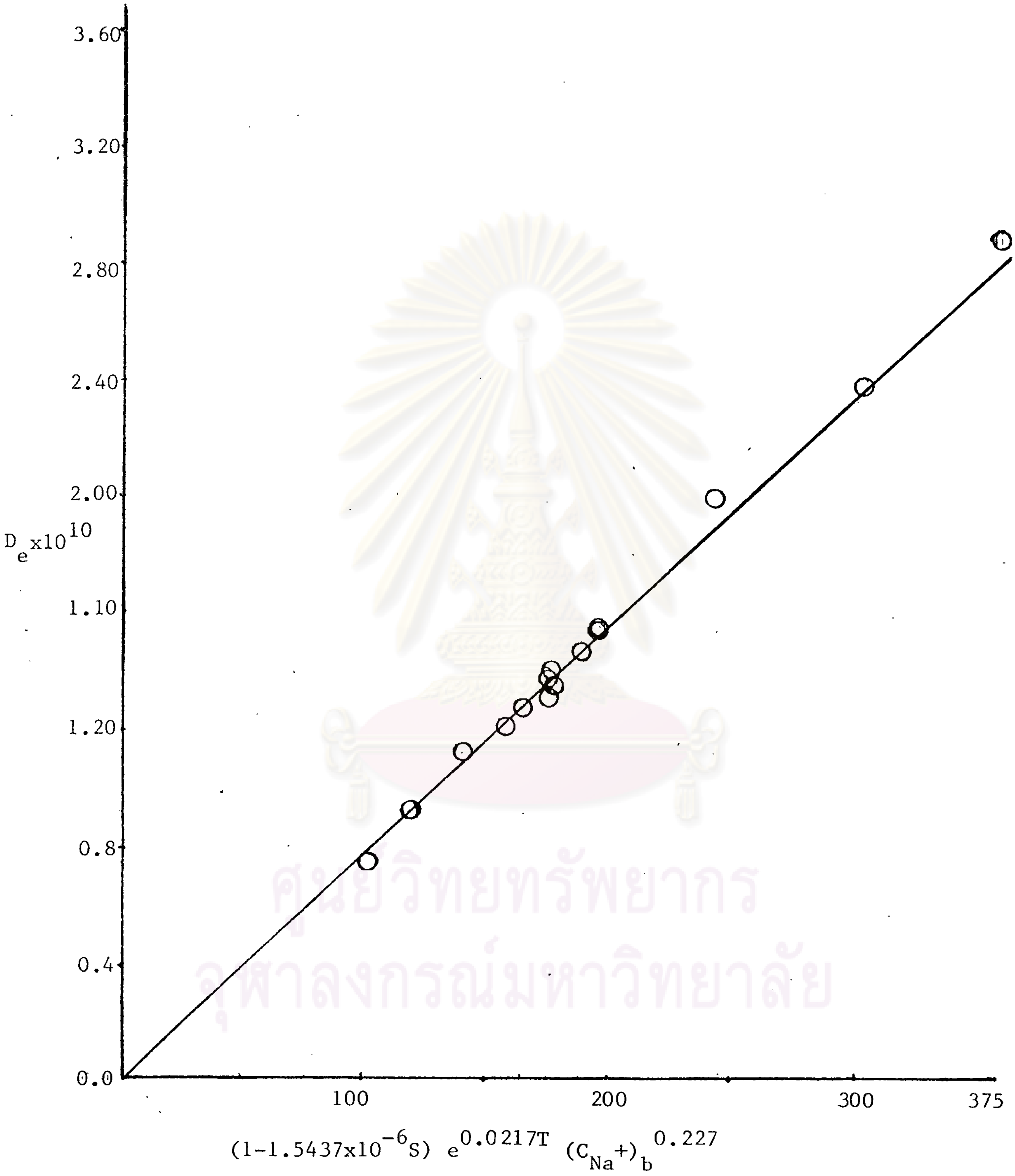

Fig 5.11 Relationship between D_e and $(1-1.5437x10^{-6}S)\ e^{0.0217T}(C_{Na^+})_b^{0.227}$